Spiral Structure and Mass Inflows In Spiral Galaxies

Yonghwi Kim, Woong-Tae Kim

CEOU, Astronomy Program, Dept. of Physics & Astronomy, Seoul National University

The 7th Korean Astrophysics Workshop on Dynamics of Disk Galaxies

October 21-24, 2013, Seoul National University, Seoul, Korea

Outline

- Discrepancy between the pitch angles of stellar and gaseous arms
- Arm extension in the gaseous medium
- Gas inflows driven by spiral arms

Arm Pitch Angles, p

Grosbol & Patsis (1998)

Galaxy	Pitch angle i_2 K′	I	V	B	Δ	range
NGC 3223	-8°.8	-9°.4	-8°.8	-8°.7	0°.5	25-36″
NGC 5085	-17°.4	-13°.0	-11°.7	-10°.9	0°.5	25-40″
NGC 5247	-34°.1	-31°.8	-29°.9	-27°.4	0°.7	30-50″
NGC 5861	-12°.4	-11°.8	-11°.9	-	0°.5	20-35″
NGC 7083	-22°.1	-20°.3	-17°.6	-15°.0	1°.0	11-18″

Red : Old Population

Blue : Young Population

- p (I- or K-band) > p (B-band)
- Overall p_{gas} is smaller by ~2°-10° than p_* for p_*~10°-30°, despite almost 1:1 correlation between them.

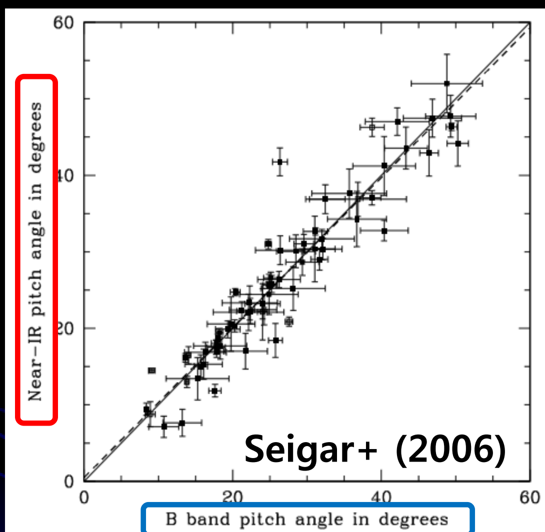

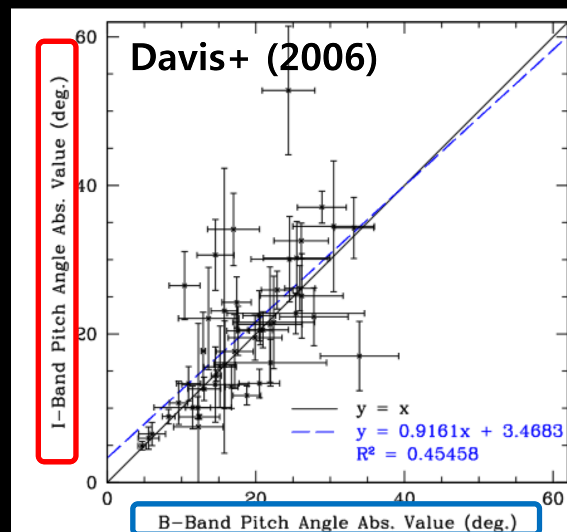

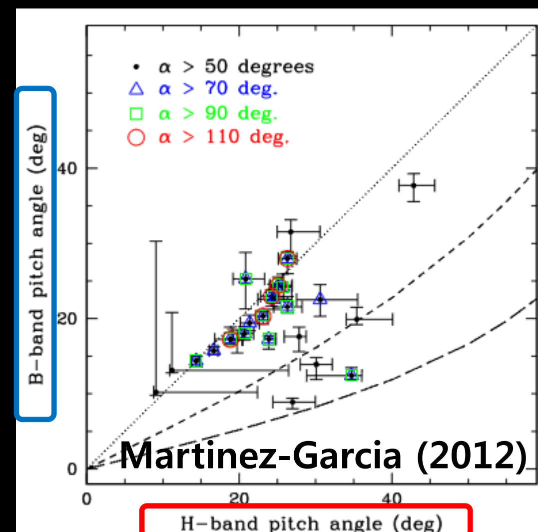

※ No convincing theoretical argument for the difference of the pitch angles between stellar and gaseous arms.

Issue

Arm Extension

- The Theory for spiral density waves
  - The stellar pattern extends up to;
    - Linear regime : corotation resonance (CR) or outer Lindblad resonance (OLR) (Toomre 1981; Lin & Lau 1979; Bertin+ 1989a,b; Zhang 1996)
    - Non-linear regime : the 4/1 resonance (Contopoulos & Grosbøl 1986, 1988; Patsis+ 1991)

※ Uncertain whether the termination of gaseous arms corresponds to the resonance radii.

Issue

Angular Momentum Transport

- Secular changes in the orbits of stars and gas clouds by spiral arms
  (Lin & Shu 1964, 1966; Toomre 1964; Elmegreen 1995; Bertin & Lin 1996; Foyle et al. 2010)
  → It leads to overall gas inflows or outflows.

- Roberts & Shu (1972, see also Kalnajs 1972)
  - Damping timescale due to the angular momentum exchange : ~1Gyr
- Lubow et al. (1986)
  - Gas accretion rate : $dM/dt=0.2\sim0.4M_{\odot}yr^{-1}$ (solar neighborhood)
  - Consistent to the results of chemical modeling by Lacey & Fall (1985)
- Hopkins & Quataert (2011)
  - Epicycle approximation to derive an analytic expression for dM/dt

※ Regarding angular momentum transport in these studies,
- Ignored the self-gravitational torque under the local approximation.
- Not considered the effects of gas pressure
- Difficult to isolate the sole effect of the shock

Issue

Main Purpose of This Study

Using global hydrodynamic simulations,

1. We address the pitch angles and spatial extent of gaseous arms in comparison with their stellar counterparts.

2. We study how the gas drift rate depends on physical parameters of spiral arms.

Spiral Arm Model

- Ordinary disk galaxies with a flat rotation curve of v_c=200 km s^{-1}
- Logarithmic spirals (Local analog of Lin & Shu 1964, 1966)

$$\Phi_{\rm ext}(R,\phi;t) = \Phi_0 \cos\left(m\left[\phi + \frac{\ln R}{\tan p_*} - \Omega_p t + \phi_0\right]\right)$$

  - Number of arms : m=2
  - Pitch angle of stellar pattern : p_*=20°

  - Arm strength is controlled by the dimensionless parameter

$$\mathcal{F} \equiv \frac{m\Phi_0}{v_c^2 \tan p_*}$$ with varying from 5% to 20%
(Roberts 1969; Shu, Milione, & Roberts 1973)

  - Pattern speed of the spiral arms
    a) Ω_p = 30km/s/kpc (Fast-arm Models) : CR at R=6.5kpc
    b) Ω_p = 10km/s/kpc (Slow-arm Models) : CR at R=20kpc

- Numerical Method
  - CMHOG Code (Connection Machine Higher Order Godunov)
    : Grid-based code in cylindrical geometry
  - Self-gravitating and isothermal gaseous disk without magnetic fields.

Extent and Shape of Gaseous Arms

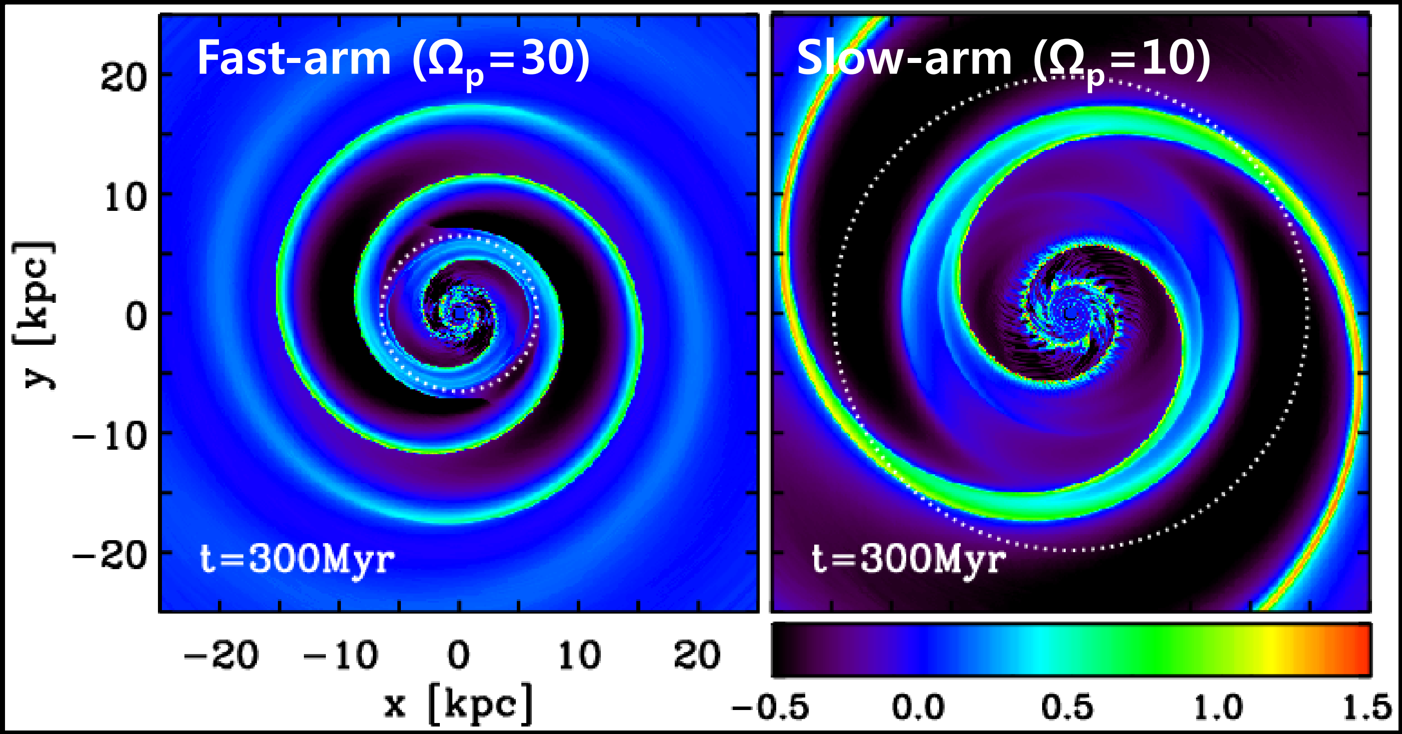

- Extension of spiral shocks
  - Fast-arm models : only up to R=18kpc
  - Slow-arm models : all the way to the outer radial boundary
- Pitch angle of gaseous arms, p_{gas}
  - Fast-arm models : $p_{gas} \ll p_*$
  - Slow-arm models : $p_{gas} \leq p_*$

Extension of Spiral Shocks

- We found empirically that quasi-steady spiral shocks exist only if

$$\boxed{\frac{t_{\rm sound}}{t_{\rm arm}} = \frac{\mathcal{M}_\perp}{\sin p_*} \lesssim 25 + 100\mathcal{F},}$$

  - Perpendicular mach number : $\mathcal{M}_\perp = \frac{R|\Omega - \Omega_s|}{c_s} \sin p_*$
  - The time interval between two successive passages of the arms : $t_{\rm arm}=\pi|\Omega-\Omega_s|$
  - The arm-to-arm sound crossing time : $t_{\rm sound}=\pi R/c_s$

- Otherwise, the gas would <u>not have sufficient time</u> to adjust itself to one arm before encountering the next arm.

  : The rapid rotation of the potential effectively makes itself smoothed significantly along the azimuthal direction.

Arm Extension in M83

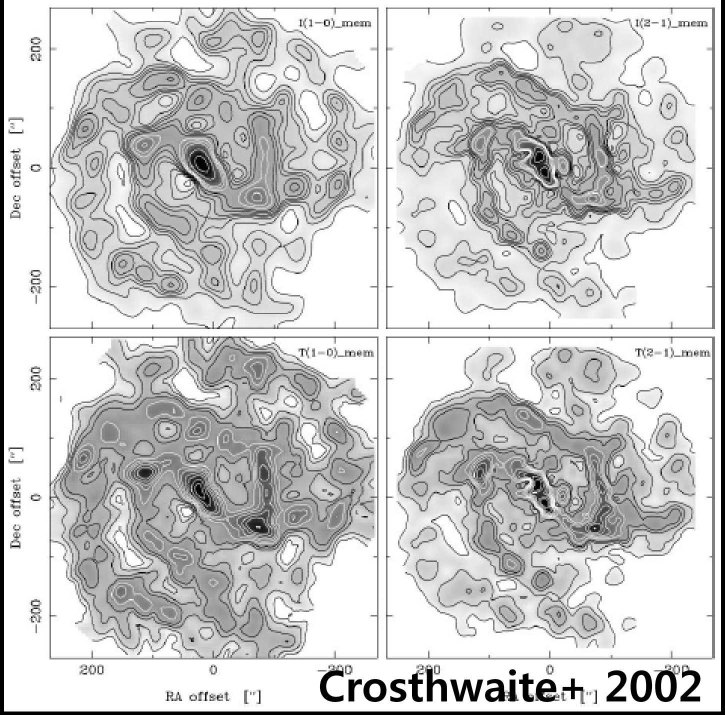

Crosthwaite+ 2002

Arm extension of M83
- R_{OLR}~5′ (Lundgren+ 2004a,b)
- R~6′ for CO & HI (Crosthwaite+ 2002)

$$\boxed{\frac{t_{\rm sound}}{t_{\rm arm}} = \frac{\mathcal{M}_\perp}{\sin p_*} \lesssim 25 + 100\mathcal{F},}$$

for $0.05 \le \mathcal{F} \le 0.2$

- The termination radius of the gaseous arms in M83 is close to the OLR.
  → Still uncertain whether the OLR plays a central role in limiting the arm extent.
- The radius of 6′ corresponds to $\boxed{\mathcal{M}_\perp / \sin p_* \sim 23\text{–}30}$.

→ The idea of arm termination by too large $M_\perp$ is not inconsistent with the observed gaseous arms in M83 with F~5-10%.

Pitch Angles of Gaseous Arms

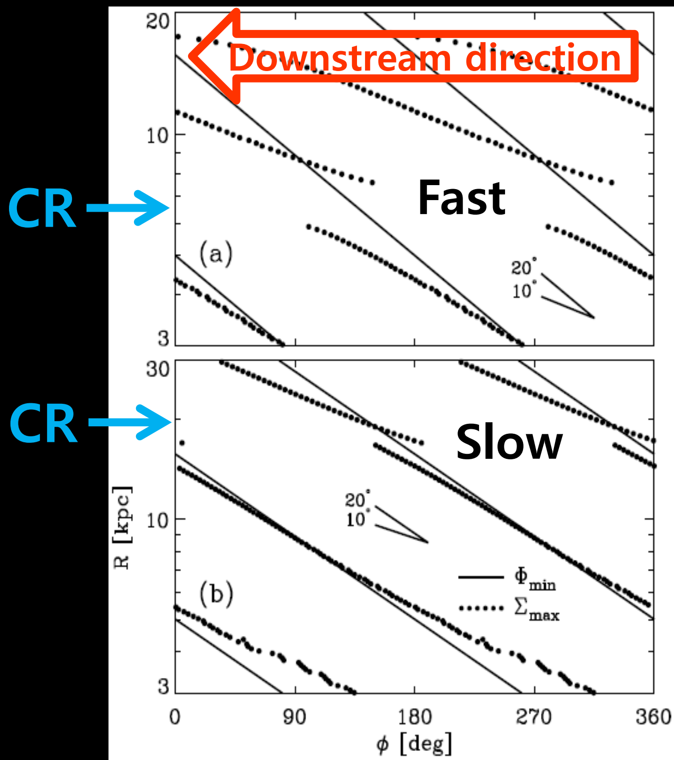

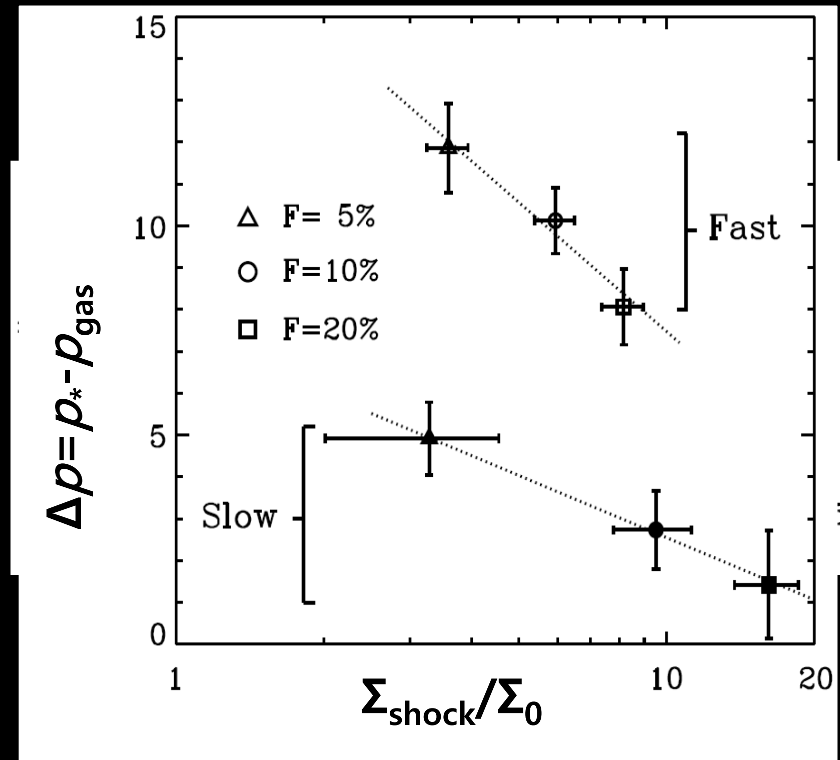

- In a quasi-steady state, stronger shock [illegible] er downstream. (Kim & Ostriker 2002; Gittins & Clarke 2004)
- In fast-arm models, $\mathcal{M}_\perp$ vary systematically large with R, leading to $p_{\rm gas} \ll p_*$.
- In slow-arm models, $\mathcal{M}_\perp < 5$, so that shocks form close to the potential minima and thus have $p_{\rm gas} < p_*$.

- The offsets between $p_{\rm gas}$ and p_*: $\Delta p = p_\star - p_{\rm gas}$
  - In general, larger $\Sigma_{\rm shock}$ corresponds to smaller Δp.
  - In the fast-arm models, $\mathcal{M}_\perp$ varies a lot with R and it has relatively weak shocks compared to the show-arm models.

Radial Dependence of Mass Drift

- Inside CR, the gas loses their L and moves radially inward.
- Outside CR, the gas gains their L and makes mass outflows.

- Inflow rates of the slow-arm models:

$\boxed{\dot{M}_{\rm tot} \approx 0.3 - 3.0\ M_{\odot}{\rm yr}^{-1}}$ for F=5-20%

$$\langle \dot{M}_{\rm tot} \rangle \approx 7\mathcal{F}(0.1 + 10\mathcal{F})(\Sigma/\Sigma_0)\,{\rm M}_{\odot}\,{\rm yr}^{-1}$$

cf. Lubow et al. (1986)'s local models yield $\dot{M} \approx 0.2 - 0.4\ M_{\odot}{\rm yr}^{-1}$ corresponding to F=3%.

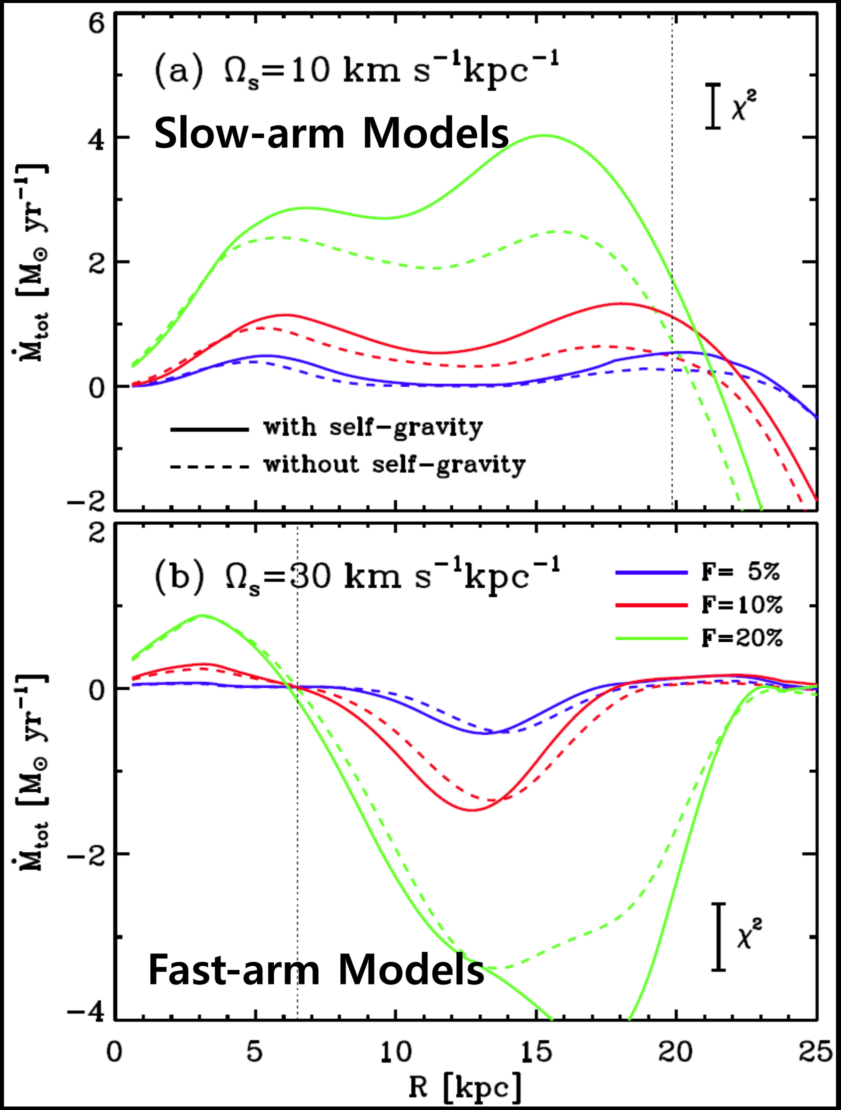

Mass Inflows

- The radial drift of the gas

  Combination of three processes:

$$\dot{M}_{\rm tot} = \dot{M}_{\rm shock} + \dot{M}_{\rm ext} + \dot{M}_{\rm self}$$

1) Dissipation of angular momentum at spiral shocks : $\dot{M}_{\rm shock}$
   (Lubow+ 1986; Hopkins & Quataert 2011)

2) Torque by the external spiral potenital (Lubow et al. 1986)

$$\dot{M}_{\rm ext} = -\left(\frac{1}{R}\frac{\partial R^2\Omega}{\partial R}\right)^{-1}\int_{-\pi}^{\pi}\Sigma\frac{\partial\Phi_{\rm ext}}{\partial\phi}d\phi$$

3) Torque by the self-gravitational potential

$$\dot{M}_{\rm self} = -\left(\frac{1}{R}\frac{\partial R^2\Omega}{\partial R}\right)^{-1}\int_{-\pi}^{\pi}\Sigma\frac{\partial\Phi_{\rm gas}}{\partial\phi}d\phi$$

Mass Inflow Rate in Slow-Arm Models

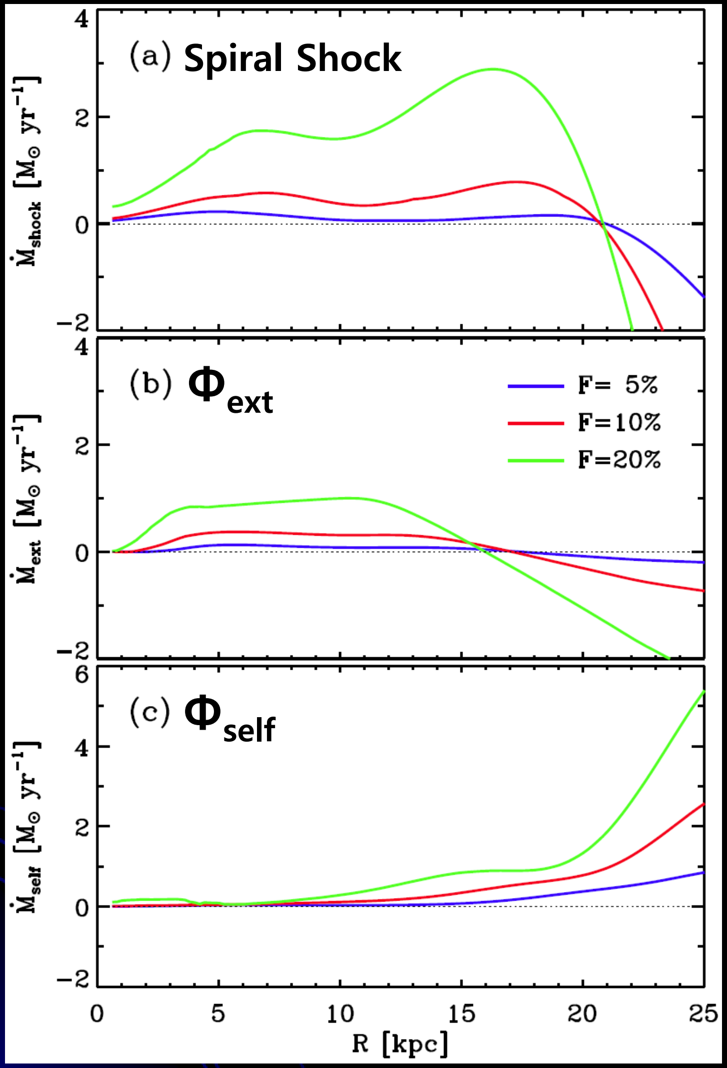

- $\dot{M}_{\rm shock} > 0$ inside the CR, as expected.
- $\dot{M}_{\rm shock} : \dot{M}_{\rm ext} : \dot{M}_{\rm self}$

  $$= 50\% : 40\% : 10\%$$

  (Averaged values over 5<R<15kpc)
- Torque by the self-gravity on the gas overwhelms the others outside the CR.

  ⇒ This is because the Toomre Q parameter is smaller at larger R.

Gravitational Torque Analysis

- NGC 4597 from HI gas observation (Garcia-Burillo et al. 2009)
  - The gravitational potential is computed on the NIR images.
  - They calculated the mass drift rate from this potential and column density of HI.

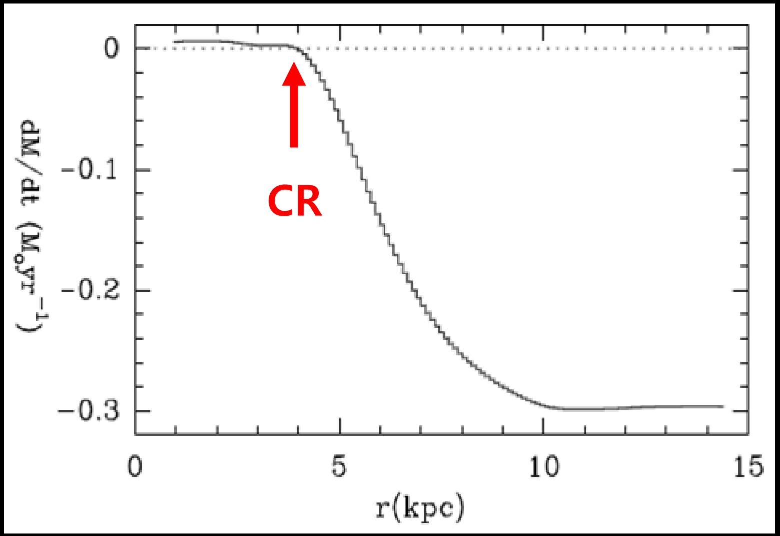

Haan et al. (2009)

Table 9
Gravitational Torque Analysis

Source	⟨dL/L⟩ H I	⟨dL/L⟩ CO	⟨|dL/L|⟩ H I	⟨|dL/L|⟩ CO	$dM_{\rm HI}/dt$ ($M_\odot$ yr^{-1})	$dM_{\rm mol}/dt$ ($M_\odot$ yr^{-1})	$R_{\rm max,HI}$ (kpc)	$R_{\rm max,CO}$ (kpc)
NGC 3368	0.02	−0.50	0.12	0.55	0.04	−11.11	13.0	0.35
NGC 3627	−0.00	0.16	0.26	0.24	−0.10	50.13	6.0	0.75
NGC 4321	0.01	0.02	0.10	0.10	−0.18	1.03	18.0	1.2
NGC 4736	0.02	0.01	0.03	0.09	0.06	−0.01	8.5	0.62
NGC 5248	0.06	−0.02	0.13	0.02	0.49	−22.96	20.5	0.8
NGC 6951	−0.04	−0.05	0.09	0.10	−0.16	−4.29	29.0	1.0
NGC 7217	−0.01	−0.02	0.03	0.03	−0.01	−2.37	15.2	1.4

Summary

- Morphologies
  - Arm extension in the gaseous medium
    - The extent of spiral shocks is limited by too large $M_{\perp}$, especially in fast-arm models.
  - Arm pitch angle
    - The arm pitch angle of gaseous arms is in general smaller than that of the stellar arms.
- Dynamics
  - Gas inflows/outflows by spiral shocks
    - Spiral arms can be efficient to transport the gas from outside to the central region at a rate $dM_{tot}/dt \sim 0.3\text{-}3.0 M_{\odot} yr^{-1}$, provided that the spiral arms have quite low Ω_p so as to have a large CR radius.
    - The inflowing gas will increase the mass in the galactic center, possibly fueling star formation.

→ It would be interesting to study how star formation is enhanced in nuclear rings by addition of outer spiral arms.

⇒ Talk by Woo-Young Seo

Thank You